



Original article

Discovery of new 7-substituted-4-imidazolylmethyl coumarins and 4'-substituted-2-imidazolyl acetophenones open analogues as potent and selective inhibitors of steroid-11 β -hydroxylase



Angela Stefanachi ^{a,*}, Nina Hanke ^b, Leonardo Pisani ^a, Francesco Leonetti ^a,
Orazio Nicolotti ^a, Marco Catto ^a, Saverio Cellamare ^a, Rolf W. Hartmann ^b, Angelo Carotti ^a

^a Dipartimento di Farmacia-Scienze del Farmaco, Università degli Studi di Bari "Aldo Moro", Via Orabona 4, 70125 Bari, Italy

^b Pharmaceutical and Medicinal Chemistry, Saarland University & Helmholtz Institute for Pharmaceutical Research Saarland (HIPS), PO Box 15 11 50, D-66041 Saarbrücken, Germany

ARTICLE INFO

Article history:

Received 28 May 2014

Received in revised form

4 September 2014

Accepted 9 October 2014

Available online 13 October 2014

Keywords:

CYP11B1 inhibitors

CYP11B2

CYP19

CYP17

Coumarins

Imidazolyl-acetophenones

ABSTRACT

Diseases triggered by an abnormally high level of cortisol (hypercortisolism), such as the Cushing's and metabolic syndromes, could be successfully tackled by inhibitors of CYP11B1, a steroidal cytochrome P450 enzyme that catalyzes the last hydroxylation step of the cortisol biosynthesis. Structural optimization of 7-(benzyloxy)-4-(1*H*-imidazol-1-ylmethyl)-2*H*-chromen-2-one **2**, a selective aromatase inhibitor, afforded the 4-(1*H*-imidazol-1-ylmethyl)-7-[[3-(trifluoromethoxy)benzyl]oxy]-2*H*-chromen-2-one **7**, with improved inhibitory potency at human CYP11B1 (IC_{50} = 5 nM) and an enhanced selectivity over human CYP11B2 (SIB = 25) compared to lead compound **2** (IC_{50} = 72 nM, SIB = 4.0) and metyrapone (IC_{50} = 15 nM, SIB = 4.8), a non-selective drug used in the therapy of the Cushing's syndrome. Structure–activity relationship studies allowed the design and optimization of a novel series of potent and selective compounds, that can be regarded as open analogues of 2*H*-chromen-2-one derivatives. Compound **23**, 2-(1*H*-imidazol-1-yl)-1-(4-[[3(trifluoromethoxy)benzyl]oxy]phenyl) ethanone, was the most interesting inhibitor of the series displaying a high potency at CYP11B1 (IC_{50} = 15 nM), increased selectivities over CYP11B2 (SIB = 33), CYP19 (SIB = 390) and CYP17 (5% inhibition at 2.5 μ M concentration).
© 2014 Elsevier Masson SAS. All rights reserved.

1. Introduction

Cytochromes P450 (CYPs) are iron-containing monooxygenase enzymes (hemoproteins) that catalyze the oxidation of exogenous and endogenous organic substances. CYPs play a pivotal role in the metabolism of xenobiotics, and drugs in particular, being responsible for their bio-activation, -toxication, -detoxification and total-body clearance processes [1]. Moreover, CYPs regulate the biosynthesis of endogenous molecules, including steroid hormones that in many diseases are over-produced and sustain the growth of cancer cells, as in estrogen- and androgen-dependent breast and prostate tumors, or induce visceral obesity, hypertension, and diabetes as in

the Cushing's and metabolic syndromes outlined by an excessive production of cortisol (hypercortisolism) [2].

Indeed potent and selective inhibitors of targeted CYPs have been extensively pursued and many efficient drugs discovered. Aromatase (CYP19) [3–5] and 17 β -hydroxylase/17,20-lyase (CYP17) [6] inhibitors are well known examples of CYPs inhibitors largely used in breast and prostate cancer, respectively (Chart 1).

More recently, two additional CYP enzymes, namely, steroid 11 β -hydroxylase (CYP11B1) [7–10] and aldosterone synthase (CYP11B2) [11–13], both involved in the biosynthesis of corticosteroid hormones, have been exploited as possible druggable targets. CYP11B1 catalyzes the last step of cortisol biosynthesis, that is the hydroxylation of 11-deoxycortisol to cortisol, whereas CYP11B2 catalyzes the conversion of 11-deoxycorticosterone to corticosterone, 18-hydroxycorticosterone and finally to aldosterone (Scheme 1).

Selective CYP11B1 inhibitors may therefore represent potential therapeutic agents for those pathologies characterized by an over-production of cortisol, like the Cushing's and metabolic syndromes [14,15]. Although metyrapone (Chart 2), a strong inhibitor of

Abbreviations: CYP, cytochrome P450; SAR, structure–activity relationship; SSR, structure–selectivity relationship; QSAR, quantitative structure–activity relationship; CYP19, aromatase; CYP17, 17 β -hydroxylase/17,20 lyase; CYP11B1, steroid 11 β -hydroxylase; CYP11B2, aldosterone synthase.

* Corresponding author.

E-mail address: angela.stefanachi@uniba.it (A. Stefanachi).

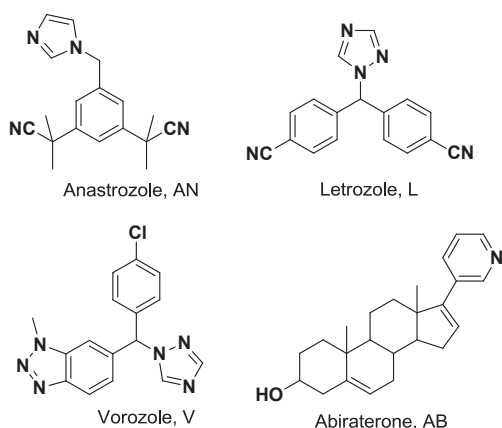


Chart 1. CYP19 (AN, L, V) and CYP17 (AB) inhibitor drugs used in the therapy of breast and prostate cancer, respectively.

CYP11B1, is in clinical use for the treatment of Cushing's syndrome, its low selectivity over aldosterone synthase CYP11B2 and the consequent block of aldosterone biosynthesis leading to severe hypokalemia and water retention, limits its therapeutic applicability [16,17].

Consequently, nowadays more selective CYP11B1 inhibitors are eagerly pursued. Unfortunately, the discovery of highly selective CYP11B1 inhibitors is not a simple task because the two CYP enzymes present a very high sequence homology and, moreover, the lack of experimental 3D models prevents the use of structure-based approaches for the design of potent and selective inhibitors. Pharmacophore and 3D QSAR models have been recently developed [18–21], but the relatively limited molecular diversity explored might preclude their sound application in the design of completely novel and selective inhibitors. Despite these objective drawbacks, careful evaluation of the structure-activity and structure-selectivity relationships (SAR and SSR, respectively) allowed the discovery of potent and highly selective CYP11B2 [21–25] and potent but slightly selective CYP11B1 inhibitors [7–10]. Two of the best compounds discovered in recent studies (e.g., A [8] and B [14] in Chart 2) displayed very good to moderately potent CYP11B1

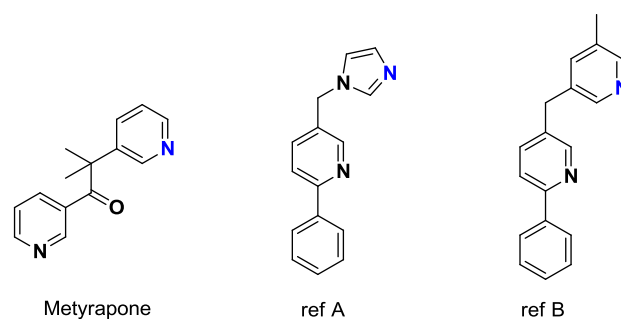


Chart 2. Chemical structures of potent and moderately selective CYP11B1 (see Table 2).

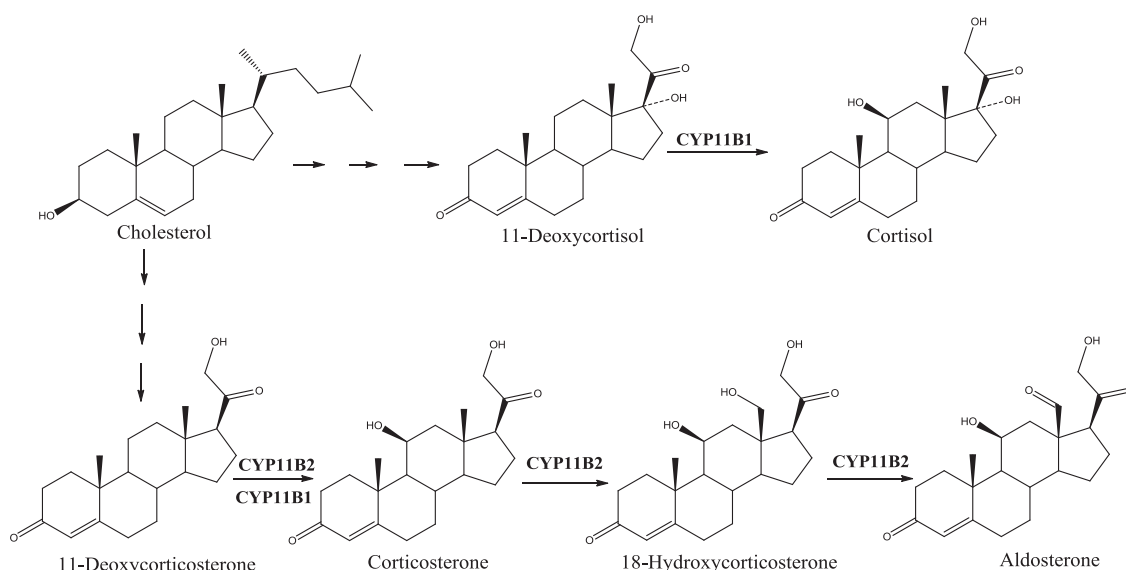
inhibition ($IC_{50} = 2$ and 107 nM, respectively) and moderate selectivity indices ($SIB = 13.3$ and 16.5 , respectively; $SIB = IC_{50}$ CYP11B2/ IC_{50} CYP11B1) but greater than that observed for metyrapone ($SIB = 4.8$) [14]. To discover novel and more potent CYP11B1 inhibitors, with a higher selectivity over CYP11B2, and CYP17 and CYP19 as well, a new research project was conceived stemming from 7-substituted-4-(imidazolylmethyl) coumarins recently reported by us as potent CYP19 inhibitors with high selectivity over CYP17 [26,27].

1.1. Chemistry

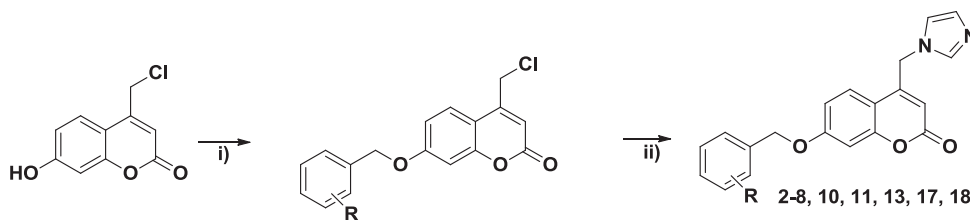
Already published coumarin derivatives **2–8**, **10**, **11**, **13**, **17** and **18** [27] were prepared from 4-(chloromethyl)-7-hydroxycoumarin through the benzylation of its phenolic group followed by the nucleophilic displacement of the chlorine atom with imidazole, according to the reaction pathway illustrated in Scheme 2.

The newly designed coumarins **9**, **12**, **14–16**, **19** and **20** were synthesized from 4-(imidazolylmethyl)-7-hydroxycoumarin [27] through a Mitsunobu reaction with the appropriate benzyl alcohol affording the desired products with high yields (Scheme 3).

The 4'(or 3')-phenyl(pyridinyl)methoxy-2-imidazolyl-acetophenones **21–27** were obtained from the 4(or 3)-hydroxy-bromoacetophenone through the nucleophilic substitution of the bromo atom with imidazole, followed by a nucleophilic reaction of the 7-OH group with an (hetero)arylmethyl bromide (Scheme 4).



Scheme 1. Biosynthesis of Cortisol and Aldosterone from Cholesterol.



Scheme 2. Reagents and conditions: i) (Substituted)benzyl bromides, K_2CO_3 , dioxane, reflux, 4 h; ii) Imidazole, CH_3CN , reflux, 2 h.

2. Results and discussion

CYP11B1 and CYP11B2 inhibition data were first determined on the two lead compounds **1** and **2** from the two classes of molecules already examined as CYP19 and CYP17 inhibitors [27]. 7-benzyloxy-4-imidazolylmethyl coumarin **2** resulted a more potent inhibitor than the corresponding 7-phenoxy analogue **1** (Table 1) and therefore, previously synthesized 7-benzyloxy coumarin derivatives **8**, **10**, **11**, **13**, **17** and **18** [27], were selected and evaluated as inhibitors at CYP11B1 and CYP11B2 along with a novel series of 7-substituted-4-imidazolylmethyl coumarins **9**, **12**, **14**–**16**, **19** and **20** in Table 2, carrying different substituents at position 7, and designed to better explore the SAR and SSR of CYP11B1, CYP11B2 and, to a lesser extent, CYP17 and CYP19 inhibition.

Results in Table 2 nicely support our intuition showing that our design of more potent and selective CYP11B1 inhibitors was successful. Unfortunately the compounds maintained a good inhibition of CYP19 and therefore the CYP11B1 over CYP 19 selectivity was low as assessed by selectivity indices SIC ($SIC = IC_{50}CYP19/IC_{50}CYP11B1$), which were always <10 with the exception of the 3- and 4- trifluoromethoxy- and the 4-isopropoxy-benzyloxy derivatives **7**, **11** and **15** ($SIC = 41$, 19 and 12 , respectively).

A rapid glance at the IC_{50} and SI data span and distribution (Table 2) revealed the exploration of a limited range of affinity and selectivity, despite the appropriate span of lipophilic, electronic and steric parameters of the selected substituents. Unfortunately, while the derivation of reliable QSAR models was precluded, highly significant insights were gained from the analysis of the salient features of SAR and SSR.

Inhibitory potency at the CYP11B2 was always lower than that observed at the CYP11B1 ($SIB > 1$) with the exception of the *para*-nitrobenzyloxy derivative **12** which presented an IC_{50} at CYP11B2 equal to 86 nM vs 111 nM at CYP11B1 ($SIB = 0.78$).

The *meta*-substituted-benzyloxy derivatives **6**, **7** and **8** resulted the most active CYP11B1 inhibitors ($IC_{50} = 20$, 5 and 20 nM, respectively) being the *meta*-trifluoromethoxy derivative **7** the most potent inhibitor of the whole examined series of molecules. Lipophilic and electron-withdrawing *meta* substituents in compounds **3**–**9** increased the inhibitory potency of lead compound **2** whereas a similarly clear trend was not observed for the *para*-substituted benzyloxy derivatives **10**–**16** which were slightly less

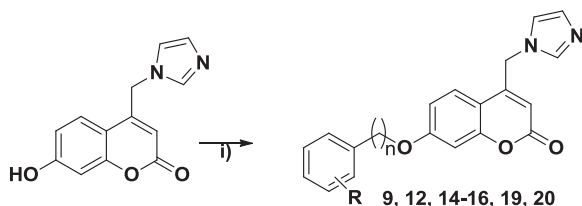
potent than the corresponding *meta*-substituted congeners. Interestingly, as for the *meta* derivatives, the *para*-trifluoromethoxybenzyloxy derivative **11** was the most potent CYP11B1 inhibitor ($IC_{50} = 20$ nM) within this sub-series of compounds whereas the bulky and highly lipophilic phenetyloxy derivative **16** showed the lowest inhibition at the CYP11B1 ($IC_{50} = 258$ nM). The di-substituted benzyloxy derivatives **17**, **18** and **19** and the trimethoxybenzyloxy-derivative **20** displayed comparable affinity at CYP11B1 regardless of the substitution pattern and the lipophilic and electronic characters of the substituents.

To further improve potency and selectivity and to gain further insights on the SAR and SSR, a small series of (3')4'-benzyloxy-2-imidazolyl-acetophenone derivatives **21**–**26**, that can be seen as open and more flexible analogues of the examined coumarin derivatives (Chart 3), was designed, prepared and tested along with the 4'-pyridinylmethoxy-2-imidazolyl-acetophenone derivative **27**. As shown in Chart 4 coumarins and open analogues did share a number of putative pharmacophoric elements.

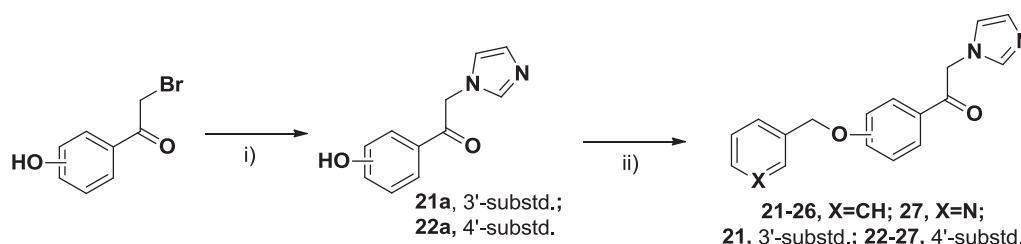
Meta-benzyloxy derivative **21** resulted almost inactive at the four tested CYPs whereas the *para*-benzyloxy lead compound of this series (**22**) showed a moderate inhibitory activity at the CYP11B1 ($IC_{50} = 149$ nM) and a poor selectivity over CYP11B2 ($SIB = 3.9$). The lower CYP11B1 inhibitory activity of compound **21** compared to its regioisomer **22** can be easily interpreted by a structural comparison with the active coumarin analogue **2** indicating a perfect overlay of putative pharmacophoric elements with compound **21** (Chart 4) that was not observed with compound **22** represented in two different low energy conformers in Chart 4. The pyridinyl isoster **27** of lead compound **22** exhibited even poorer potency and selectivity ($IC_{50} = 518$ nM; $SIB = 2.7$) suggesting that the polar and electron rich pyridine ring was poorly tolerated in a likely hydrophobic binding region of CYP11B1.

The *meta*-substituted-benzyloxy derivatives **23**–**25** and, to a lesser extent, the *para*-substituted benzyloxy derivative **26**, exhibited inhibitory potency at CYP11B1 and selectivity over CYP11B2 greater than lead compound **22**. Very interestingly, analogously to what was observed in the coumarin series (see compound **7**), the *meta*-trifluoromethoxybenzyl derivative **23** exhibited a high potency at the CYP11B1 ($IC_{50} = 15$ nM) and good selectivities over CYP11B2 and CYP 19 ($SIB = 33$ and $SIC = 390$).

The high structural analogy between the coumarins and the open analogues (see Charts 3 and 4) led to hypothesize a similar binding mode at both CYP11B1 and CYP11B2. However, some different interactions did take place at the two enzyme binding sites as proved by the good selectivity displayed by a number of inhibitors, e.g., **23**, **7**, and **11**. As these compounds were characterized by the presence of hydrophobic and electron-withdrawing substituents, one may speculate that hydrophobic and polar interactions favored by electron-withdrawing groups (π - π interactions?) might trigger different interaction energies at the two likely different binding sites.



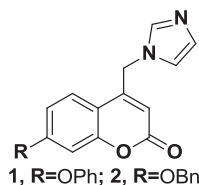
Scheme 3. Reagents and conditions: i) (Substituted)benzyl alcohols, PPh_3 , DIAD, dry THF, r.t., 18 h.



Scheme 4. Reagents and conditions: i) Imidazole, CH₃CN, reflux, 2 h; ii) (Hetero)arylmethyl bromide, K₂CO₃, dioxane, reflux, 4 h.

Table 1
CYP Inhibition data of compounds **1** and **2**.

Comps	CYP19 Inhibition ^{a,b} IC ₅₀ , nM	CYP17 % Inhibition ^{a,c} at 2.5 μM	CYP11B1 Inhibition ^{a,d} IC ₅₀ , nM	CYP11B2 Inhibition ^{a,d} IC ₅₀ , nM
1	47	14%	933	2190
2	150	3%	72	289



^a Mean value of two or three experiments with a standard error always <15%.

^b Human placental CYP19; substrate androstenedione, 500 nM.

^c E. coli expressing human CYP17; substrate progesterone, 2.5 μM.

^d Hamster fibroblasts expressing human CYP11B1 or CYP11B2; substrate 11-deoxycorticosterone, 100 nM.

Finally, to evaluate the possibility to progress some of our compounds towards pre-clinical studies, selected physicochemical and pharmacokinetic parameters were estimated by QikProp [28] for compounds **2**, **7**, **22** and **23** (Table 3). The calculated values suggested that both classes of compounds have a good druglikeness with comparable physicochemical properties such as aqueous solubility and octanol/water partition coefficient (compare **2** vs **22** and **7** vs **23**). Estimated pharmacokinetic parameters looked instead slightly improved for the open analogues that showed cell permeability in the Caco-2 cells (model for the gut blood barrier) and MDCK cells (model for the blood brain barrier always higher than the corresponding coumarin analogues, i.e., **22** > **2** and **23** > **7**). The 4'-substituted-2-imidazolyl acetophenone open analogues can be therefore seen as promising pre-clinical candidates for further development.

3. Conclusions

Cushing's syndrome, a disease characterized by an excessive production of cortisol, is generally treated with metyrapone, a non-selective CYP11B1 inhibitor. The lack of selectivity over CYP11B2 and other cytochromes P450, such as CYP19 and CYP17, brings about unwanted and severe side effects that strongly limit the therapeutic use of metyrapone.

The discovery of more potent and selective CYP11B1 inhibitors was one of the main goal reached in the present work. Structural optimizations of 7-benzyloxy coumarin derivative **2** led to compound **7** that exhibited an outstanding potency at CYP11B1 (IC₅₀ = 5 nM) and good selectivity over CYP11B2 and CYP19 (SIB = 25 and SIC = 41, respectively) that represented a net improvement over metyrapone (IC₅₀ = 15 nM; SIB = 4.8). Moving from the coumarin derivatives to the benzyloxy-benzoylmethyl imidazole analogues afforded the potent CYP11B1 inhibitor **23** (IC₅₀ = 15 nM) that showed a further improvement of the selectivity index over CYP11B2 (SIB = 33). Very interestingly, this compound exhibited also a very high selectivity over CYP19 (SIC = 390)

and an extremely high selectivity over CYP17, which was not significantly inhibited (5%) at 2.5 μM concentration. Its interesting potency and selectivity profiles, may warrant further in vitro and in vivo investigation in animal model of Cushing's syndrome.

Finally, the limited, but significant insights gained in the analysis of the SAR and SSR might drive further optimizations of compound **7** and **23** and suggest appropriate scaffold hopping from coumarins to other bicyclic and/or tricyclic heteroaromatics advocated also by the safety concerns recently raised on coumarins-containing biological active agents [29–31]. We are currently working along such a research line and the results will be presented in due course.

4. Experimental section

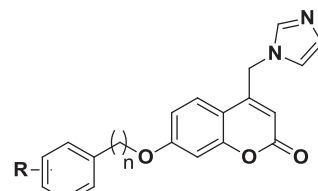
4.1. Chemistry

High analytical grade chemicals and solvents were from commercial suppliers (Sigma–Aldrich 3050 Spruce St. St. Louis MO 63103 USA, Alfa Aesar 26 Parkridge Rd Ward Hill MA 01835 USA and VWR Radnor Corporate Center, Building One, Suite 200, 100 Matsonford Road, Radnor, PA 19087).

Thin-layer chromatography (TLC) was performed on aluminum sheets pre-coated with silica gel 60 F254 (0.2 mm) type (E. Merck). Chromatographic spots were visualized by UV light. Purification of crude compounds was carried out by flash column chromatography on silica gel 60 (Kieselgel 0.040–0.063 mm, E. Merck) or by crystallization. Melting points (uncorrected) for fully purified products (see below) were determined in a glass capillary tube on the Stuart Scientific electrothermal apparatus SMP3.

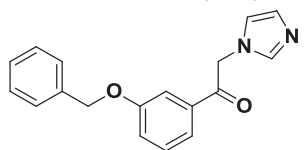
¹H NMR spectra were recorded in CDCl₃ (unless otherwise indicated) at 300 MHz on a Varian Mercury 300 instrument. All the detected signals were in accordance with the proposed structures. Chemical shifts (δ scale) are reported in parts per million (ppm) relative to the central peak of the solvent. Coupling constant (*J* values) are given in hertz (Hz). Spin multiplicities are given as: s (singlet), d (doublet), dd (double doublet), t (triplet), ept (eptuplet)

Table 2
CYP Inhibition and selectivity data of compounds 2–27.



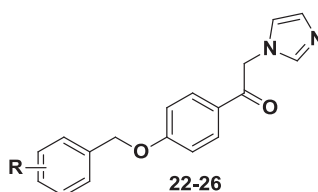
2-20

Comps	R	n	CYP11B1 IC ₅₀ nM ^{a,b}	CYP11B2 IC ₅₀ , nM ^{a,b}	SIB ^c	CYP17 % inhibition ^{a,d}	CYP19 IC ₅₀ , nM ^{a,e}	SIC ^f
2	H	1	72	289	4.1	3%	150	2.1
3	3-CH ₃	1	45	250	5.6	0%	114	2.5
4	3-F	1	40	200	5.0	0%	113	2.8
5	3-Cl	1	31	101	3.3	3%	130	4.2
6	3-CF ₃	1	20	150	7.5	0%	235	12
7	3-OCF ₃	1	5	125	2.5	3%	207	41
8	3-NO ₂	1	20	100	5.0	3%	141	7.1
9	3-OCH ₃	1	48	127	2.6	2%	549	11
10	4-Cl	1	100	200	2.0	1%	178	1.8
11	4-OCF ₃	1	25	250	10	1%	481	19
12	4-NO ₂	1	111	86	0.78	1%	387	3.5
13	4-OCH ₃	1	80	124	1.5	1%	127	1.6
14	4-OCH ₂ CH ₂ CH ₃	1	63	77	1.2	2%	477	7.6
15	4-OCH(CH ₃) ₂	1	48	82	1.7	2%	584	12
16	H	2	258	899	3.5	2%	639	2.5
17	3,5-F ₂	1	45	200	4.4	2%	169	3.8
18	3,4-F ₂	1	50	100	2.0	1%	165	3.3
19	3,4-(OCH ₃) ₂	1	57	82	1.4	0%	445	7.8
20	3,4,5-(OCH ₃) ₃	1	50	147	2.9	2%	349	7.0



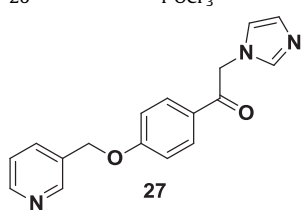
21

Comps	R	CYP11B1 IC ₅₀ nM ^{a,b}	CYP11B2 IC ₅₀ , nM ^{a,b}	SIB ^c	CYP17 % inhibition ^{a,d}	CYP19 IC ₅₀ , nM ^{a,e}	SIC ^f
21	–	>500	>500	–	1%	17464	–nd



22-26

Comps	R	CYP11B1 IC ₅₀ nM ^{a,b}	CYP11B2 IC ₅₀ , nM ^{a,b}	SIB ^c	CYP17 % inhibition ^{a,d}	CYP19 IC ₅₀ , nM ^{a,e}	SIC ^f
22	H	149	588	3.9	1%	4490	30
23	3-OCF ₃	15	497	33	5%	5855	390
24	3-NO ₂	24	192	8.0	5%	3708	155
25	3-CN	30	222	7.4	3%	4566	152
26	4-OCF ₃	109	669	6.1	0%	8299	76



27

Comps	R	CYP11B1 IC ₅₀ nM ^{a,b}	CYP11B2 IC ₅₀ , nM ^{a,b}	SIB ^c	CYP17 % inhibition ^{a,d}	CYP19 IC ₅₀ , nM ^{a,e}	SIC ^f
27	–	518	1397	2.7	6%	31813	61
Metyrapone	–	15	72	4.8	3%	0	nd
Ref A ⁸	–	107	1423	13.3	2%	0	nd

Table 2 (continued)

Ref B ¹⁴	2	33	16.5	5%	1%	nd
---------------------	---	----	------	----	----	----

^a Mean value of two or three experiments with a standard error always <15%.

^b Hamster fibroblasts expressing human CYP11B1 or CYP11B2; substrate 11-deoxycorticosterone, 100 nM.

^c SIB: IC₅₀CYP11B2/IC₅₀ CYP11B1.

^d *E. coli* expressing human CYP17; substrate progesterone, 2.5 μM except for ref. A and B (2.0 μM).

^e Human placental CYP19; substrate androstenedione, 500 nM.

^f SIC: IC₅₀ CYP19/IC₅₀ CYP11B1; nd, not determinable. Reference compounds, ketoconazole IC₅₀, 4.5 μM for CYP17 and **2** IC₅₀, 0.15 μM for CYP19.

and m (multiplet). ESI-MS was performed with an Electrospray interface Ion Trap Mass spectrometer (1100 series LC/MSD Trap System Agilent, Palo Alto, Ca).

The purity of all the intermediates, checked by ¹H NMR and HPLC, was always higher than 90%. Purity of all the tested final products, determined by analytical HPLC by means of a peak area normalization method, was always greater than 95%. Reverse phase HPLC analyses were performed on a system equipped with automatic injector and a Waters Breeze 1525 high performance liquid chromatography (HPLC) pump coupled with a Waters 2489 UV Detector (Waters Corporation, Milford, MA) using a Waters XTerra RP 5 μm C8 column (150 mm × 3.0 mm i. d.). The UV detection was measured at 254 and 280 nm. Each tested compound was analyzed by elution with two different mobile phase systems: in system 1, compounds were eluted using a 80/20 methanol/water mixture at a flow rate of 0.5 mL/min; in system 2, compounds were eluted using a 65/35 acetonitrile/water mixture at a flow rate of 0.5 mL/min.

4.1.1. General procedure for the synthesis of 7-(1H-imidazol-1-ylmethyl)coumarin derivatives **9**, **12**, **14**–**16**, **19** and **20**

7-Hydroxy-4-(imidazolylmethyl) coumarin (0.242 g, 1.0 mmol) was dissolved in anhydrous THF (3 mL), and then the appropriate benzyl alcohol (1.20 mmol) was added followed by PPh₃ (0.315 g, 1.20 mmol). The solution was cooled to 0 °C through an external ice bath, and a solution of DIAD (0.236 mL, 1.20 mmol) in anhydrous THF (2 mL) was added dropwise. The reaction was slowly warmed to room temperature and stirred for 18 h. The solvent was removed under reduced pressure, and the resulting crude mixture was purified by flash column chromatography (DCM/MeOH: 9.5/0.5) and the obtained residue was crystallized from absolute ethanol.

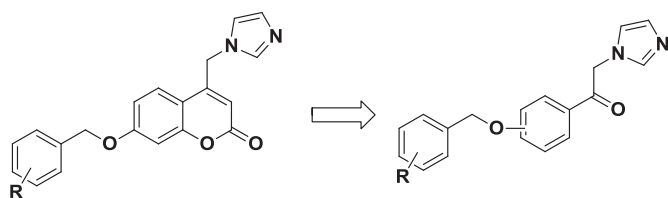


Chart 3. Design of “open coumarin analogues”: removal of molecular rigidity.

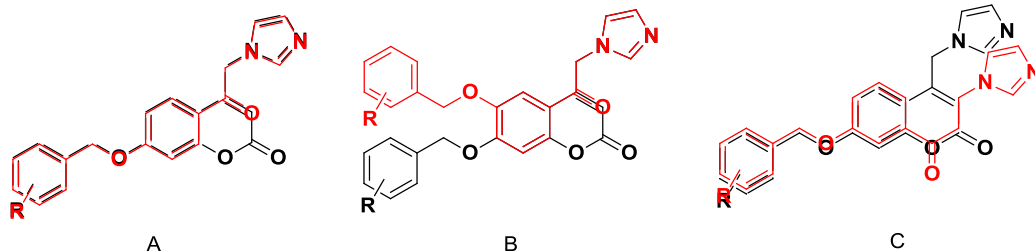


Chart 4. Overlay of low-energy conformers of 7-benzyloxy coumarins (black) and para- (A) and meta-benzyloxy-substituted (B and C) open analogues (red). (For interpretation of the references to color in this figure legend, the reader is referred to the web version of this article.)

4.1.2. 4-((1H-imidazol-1-yl)methyl)-7-((3-methoxybenzyl)oxy)-2H-chromen-2-one **9**

Yield: 69%. Mp: 146–148 °C. ¹H NMR δ: 7.59 (s, 1H), 7.41 (d, J = 8.5 Hz, 1H), 7.32 (t, J = 7.3 Hz, 1H), 7.18 (s, 1H), 7.01–6.91 (m, 6H), 5.72 (s, 1H), 5.27 (s, 2H), 5.12 (s, 2H), 3.82 (s, 3H). ESI-MS: m/z 361 [M–H][−].

4.1.3. 4-((1H-imidazol-1-yl)methyl)-7-((4-nitrobenzyl)oxy)-2H-chromen-2-one **12**

Yield: 75%. Mp: 221–223 °C. ¹H NMR δ: 8.28 (d, J = 8.5, 2H), 7.62 (d, J = 8.5, 2H), 7.59 (s, 1H), 7.40 (d, J = 8.5 Hz, 1H), 7.18 (s, 1H), 6.98–6.95 (m, 2H), 6.93–6.92 (m, 1H), 5.76 (s, 1H), 5.28 (s, 2H), 5.25 (s, 2H). ESI-MS: m/z 376[M–H][−].

4.1.4. 4-((1H-imidazol-1-yl)methyl)-7-((4-propoxybenzyl)oxy)-2H-chromen-2-one **14**

Yield: 71%. Mp: 131–133 °C. ¹H NMR (DMSO-d₆) δ: 8.12–8.08 (m, 2H), 7.75 (d, J = 8.8 Hz, 1H), 7.37 (d, J = 8.5 Hz, 2H), 7.36 (s, 1H), 7.12–7.02 (m, 2H), 6.93 (d, J = 8.5 Hz, 2H), 5.56 (s, 2H), 5.49 (s, 1H), 5.13 (s, 2H), 3.90 (t, J = 6.5 Hz, 2H), 1.74–1.67 (m, 2H), 0.95 (t, J = 7.5 Hz, 3H). ESI-MS: m/z 389 [M–H][−].

4.1.5. 4-((1H-imidazol-1-yl)methyl)-7-((4-isopropoxybenzyl)oxy)-2H-chromen-2-one **15**

Yield: 55%. Mp: 138–141 °C. ¹H NMR (DMSO-d₆) δ: 7.78–7.74 (m, 2H), 7.36 (d, J = 8.5 Hz, 2H), 7.26 (s, 1H), 7.11 (d, J = 2.4 Hz, 1H), 7.04 (dd, J = 8.9, 2.4 Hz, 1H), 6.97 (s, 1H), 6.91 (d, J = 8.5 Hz, 2H), 5.52 (s, 2H), 5.43 (s, 1H), 5.13 (s, 2H), 4.60 (ept, J = 6.0 Hz, 1H), 1.24 (d, J = 6.0 Hz, 6H). ESI-MS: m/z 389 [M–H][−].

4.1.6. 4-((1H-imidazol-1-yl)methyl)-7-phenethoxy-2H-chromen-2-one **16**

Yield: 55%. Mp: 160–162 °C. ¹H NMR δ: 7.58 (s, 1H), 7.40–7.26 (m, 5H), 7.18 (s, 1H), 6.96 (s, 1H), 6.90–6.88 (m, 2H), 5.71 (s, 2H), 5.27 (s, 2H), 4.24 (t, J = 7.2 Hz, 2H), 3.11 (t, J = 7.15 Hz, 2H). ESI-MS: m/z 345 [M–H][−].

4.1.7. 4-((1H-imidazol-1-yl)methyl)-7-((3,4-dimethoxybenzyl)oxy)-2H-chromen-2-one **19**

Yield: 71%. Mp: 118–120 °C. ¹H NMR δ: 7.64 (s, 1H), 7.41 (d, J = 8.8 Hz, 2H), 7.27–7.24 (m, 2H), 6.99–6.90 (m, 3H), 6.89 (d,

Table 3
Estimated physicochemical and pharmacokinetic parameters by QikProp [28].

Parameters	2	7	22	23	Range ^a or recommended value
QPlogPo/w ^b	3.49	4.65	3.66	4.83	–2–6.5
QPlogS ^c	–4.28	–5.81	–4.14	–5.69	–6.5–0.5
QPPCaco ^d	1017.63	1017.76	2087.83	2090.60	<25 poor >500 great
QPlogBB ^e	–0.76	–0.58	–0.52	–0.31	–3–1.2
QPPMDCK ^f	504.14	2354.85	1096.23	5127.25	<25 poor >500 great
Human oral absorption index ^g	3	3	3	3	1: low 2: medium 3: high
Percent human oral absorption ^h	100	100	100	100	<25% poor >80% great

^a For 95% of known drugs.

^b Predicted octanol/water partition coefficient.

^c Predicted aqueous solubility, log S.

^d Predicted apparent Caco-2 cell permeability in nm/sec.

^e Predicted brain/blood partition coefficient.

^f Predicted apparent MDCK cell permeability in nm/sec.

^g Predicted qualitative human oral absorption.

^h Predicted human oral absorption on 0–100% scale.

$J = 7.5$ Hz, 1H), 5.73 (s, 1H), 5.27 (s, 2H), 5.07 (s, 2H), 3.90 (s, 6H). ESI-MS: m/z 391[M–H][–].

4.1.8. 4-((1H-imidazol-1-yl)methyl)-7-((3,4,5-trimethoxybenzyl)oxy)-2H-chromen-2-one **20**

Yield: 58%. Mp: 127–129 °C. ¹H NMR δ : 7.60 (s, 1H), 7.42 (d, $J = 8.8$ Hz, 2H), 6.98–6.94 (m, 3H), 6.64 (s, 2H), 5.74 (s, 1H), 5.28 (s, 2H), 5.06 (s, 2H), 3.88 (s, 6H), 3.86 (s, 3H). ESI-MS: m/z 421[M–H][–].

4.1.9. General procedure for the preparation of 1-(3(or 4)-hydroxyphenyl)-2-(1H-imidazol-1-yl)ethanone **21a** and **22a**

Para-(or meta-)hydroxybromoacetophenone (0.430 g, 2.0 mmol) and imidazole (0.408 g, 6.0 mmol) were dissolved in acetonitrile (10 mL) and the mixture was stirred at reflux for 1 h. The solvent was evaporated to dryness and the residue was treated with water thus obtaining a white precipitate that was used in the subsequent reaction without any further purification.

4.1.10. 1-(3-Hydroxyphenyl)-2-(1H-imidazol-1-yl)ethanone **21a**

Yield: 92%. ¹H NMR (DMSO- d_6) δ : 9.88 (s, 1H), 7.55 (s, 1H), 7.42 (d, $J = 7.8$ Hz, 1H), 7.34 (s, 1H), 7.14–7.05 (m, 2H), 7.08 (s, 1H), 6.88 (s, 1H), 5.65 (s, 2H). ESI-MS: m/z 201[M–H][–].

4.1.11. 1-(4-Hydroxyphenyl)-2-(1H-imidazol-1-yl)ethanone **22a**

Yield: 75%. ¹H NMR (DMSO- d_6) δ : 10.52 (s, 1H), 7.98 (d, $J = 8.8$ Hz, 2H), 7.56 (s, 1H), 7.08 (s, 1H), 6.90 (s, 1H), 6.88 (d, $J = 8.8$ Hz, 2H), 5.60 (s, 2H). ESI-MS: m/z 201[M–H][–].

4.1.12. General procedure for the preparation of 4'(or 3')-phenyl(pyridinyl)methoxy-2-imidazolyl-acetophenones **21–27**

Intermediate **21a** or **22a** (0.050 g, 0.25 mmol) was dissolved in absolute EtOH (10 mL) and subsequently the appropriate arylmethyl bromide (0.38 mmol) and K₂CO₃ (0.051 g, 0.38 mmol) was added. The reaction was kept at reflux for 6 h under stirring. After cooling, the precipitate was filtered off, and the solution was evaporated to dryness. The crude product was purified by flash column chromatography (DCM/MeOH: 9/1).

4.1.13. 1-(3-(Benzyloxy)phenyl)-2-(1H-imidazol-1-yl)ethanone **21**

Yield 35%. Mp: 116–118 °C. ¹H NMR (DMSO- d_6) δ : 7.60–7.53 (m, 2H), 7.47–7.34 (m, 6H), 7.32–7.27 (m, 1H), 7.16–7.09 (m, 2H), 6.94 (s, 1H), 5.95 (s, 2H), 5.51 (s, 2H). ESI-MS: m/z 291[M–H][–].

4.1.14. 1-(4-(Benzyloxy)phenyl)-2-(1H-imidazol-1-yl)ethanone **22**

Yield 42%. Mp: 137–1390 °C. ¹H NMR δ : 7.75 (d, $J = 8.8$ Hz, 2H), 7.36 (s, 1H), 7.26–7.17 (m, 5H), 6.95 (s, 1H), 6.87 (d, $J = 8.8$ Hz, 2H), 6.75 (s, 1H), 5.16 (s, 2H), 4.97 (s, 2H). ESI-MS: m/z 291[M–H][–].

4.1.15. 2-(1H-imidazol-1-yl)-1-(4-((3-(trifluoromethoxy)benzyl)oxy)phenyl)ethanone **23**

Yield 43%. Mp: 87–89 °C. ¹H NMR δ : 7.97 (d, $J = 8.8$ Hz, 2H), 7.47–7.41 (m, 1H), 7.37 (s, 1H), 7.36–7.33 (m, 1H), 7.30 (s, 1H), 7.28–7.20 (m, 3H), 7.07 (d, $J = 8.8$ Hz, 2H), 5.41 (s, 2H), 5.17 (s, 2H). ESI-MS: m/z 375 [M–H][–].

4.1.16. 2-(1H-imidazol-1-yl)-1-(4-((3-nitrobenzyl)oxy)phenyl)ethanone **24**

Yield 54%. Mp: 119–121 °C. ¹H NMR δ : 8.33 (s, 1H), 8.21 (d, $J = 8.3$ Hz, 1H), 7.98 (d, $J = 8.8$ Hz, 2H), 7.78 (d, $J = 7.4$ Hz, 1H), 7.66–7.60 (m, 1H), 7.52 (s, 1H), 7.14 (s, 1H), 7.08 (d, $J = 8.8$ Hz, 2H), 6.95 (s, 1H), 5.35 (s, 2H), 5.25 (s, 2H). ESI-MS: m/z 336 [M–H][–].

4.1.17. 3-((4-(2-(1H-imidazol-1-yl)acetyl)phenoxy)methyl)benzonitrile **25**

Yield 54%. Mp: 130–132 °C. ¹H NMR δ : 7.97 (d, $J = 8.8$ Hz, 2H), 7.75 (s, 1H), 7.68–7.64 (m, 2H), 7.55–7.50 (m, 2H), 7.15 (s, 1H), 7.06 (d, $J = 8.8$ Hz, 2H), 6.95 (s, 1H), 5.35 (s, 2H), 5.18 (s, 2H). ESI-MS: m/z 340 [M+Na]⁺.

4.1.18. 2-(1H-imidazol-1-yl)-1-(4-((4-(trifluoromethoxy)benzyl)oxy)phenyl)ethanone **26**

Yield 54%. Mp: 115–117 °C. ¹H NMR δ : 7.97 (d, $J = 8.8$ Hz, 2H), 7.58 (s, 1H), 7.47 (d, $J = 8.5$ Hz, 2H), 7.26 (d, $J = 8.5$ Hz, 2H), 7.15 (s, 1H), 7.06 (d, $J = 8.8$ Hz, 2H), 6.95 (s, 1H), 5.36 (s, 2H), 5.15 (s, 2H). ESI-MS: m/z 375 [M–H][–].

4.1.19. 2-(1H-imidazol-1-yl)-1-(4-(pyridin-3-ylmethoxy)phenyl)ethanone **27**

Yield 54%. Mp: 105–107 °C. ¹H NMR δ : 8.71–8.64 (m, 3H), 7.97 (d, $J = 8.8$ Hz, 2H), 7.79 (d, $J = 7.3$ Hz, 1H), 7.37–7.35 (m, 2H), 7.08 (d, $J = 8.8$ Hz, 2H), 6.95 (s, 1H), 5.37 (s, 2H), 5.15 (s, 2H). ESI-MS: m/z 292 [M–H][–].

4.2. Biological methods

4.2.1. CYP11B1 and CYP11B2 inhibition assay

V79MZh11B1 and V79MZh11B2 cell lines were cultivated in Dulbecco's modified Eagle medium (DMEM, Sigma) supplemented with 5% of fetal calf serum (FCS; Sigma), penicillin (100 U/ml), streptomycin (100 μ g/ml), glutamine (2 mM) and sodium pyruvate (1 mM) at 37 °C in 5% CO₂ in air.

V79MZ cells expressing human CYP11B1 and human CYP11B2 genes, respectively, were grown on 24-well cell culture plates (8 \times 10⁵ cells per well) with 1.9 cm² culture area per well in 1 mL DMEM culture medium until confluence. Before testing, the DMEM culture medium was removed and 450 μ l of fresh DMEM, containing 1% of the ethanolic dilution of the inhibitor, was added to each well. Controls were treated in the same way without inhibitors. Every value was determined in duplicate. After a pre-incubation step of 60 min at 37 °C, the reaction was started by the addition of 50 μ l of DMEM containing the substrate 11-deoxycorticosterone (containing 0.15 μ Ci of [1,2-³H] 11-deoxycorticosterone, final concentration 100 nM).

The V79MZh11B1 cells were incubated for 25 min, the V79MZh11B2 cells were incubated for 45 min. The ethanol concentration in each well was 1%.

Enzyme reactions were stopped by extracting the supernatant with ethyl acetate. Samples were centrifuged (10,000× g, 10 min), and the solvent was pipetted into fresh cups. The solvent was evaporated and the steroids were redissolved in 40 µl of methanol and analyzed by HPLC.

4.2.2. CYP17 inhibition assay

Briefly, human CYP17 and rat P450 reductase are expressed in *E. coli* [32] 140 µl phosphate buffer (50 mM sodium phosphate, 1 mM MgCl₂, 0.1 mM EDTA, 0.1 mM dithiothreitol, pH 7.4), 50 µl NADPH generating system (in phosphate buffer with 10 mM NADP⁺, 100 mM glucose-6-phosphate and 0.5 units glucose-6-phosphate dehydrogenase), 5 µl of a mixture of progesterone and [³H]-progesterone (1.2475 mM + 0.0025 mM with 101.3 Ci/mmol, final concentrations in the assay 24.95 µM + 0.05 µM) and 5 µl inhibitor (in 100% DMSO) are preincubated at 37 °C for 5 min. The reaction is started by addition of 50 µl enzyme preparation (diluted approx. 1:7–1:15 to achieve a conversion of 20% of the substrate in 30 min) and stopped after 30 min incubation (37 °C) by addition of 50 µl 1 N HCl.

The steroids are extracted with 1 mL ethyl acetate (10 min shaking, followed by 5 min of centrifugation at 12500 rpm). 900 µl supernatant are transferred into new cups and washed with 250 µl phosphate buffer plus 50 µl 1 N HCl (10 min shaking, followed by 5 min of centrifugation at 12500 rpm). 800 µl are transferred into new cups. After evaporation of the ethyl acetate (SpeedVac), the steroids are redissolved in 40 µl methanol (100%). 16β-Hydroxyprogesterone, 17β-hydroxyprogesterone and progesterone are separated by HPLC using a C18 chromatography column (CC 125/3 Nucleodur 100-3 C-18 ec column, Macherey–Nagel, Düren) connected to an HPLC-system (Agilent 1100 Series, Agilent Technologies, Waldbronn). HPLC conditions are as follows: Eluent A is 0.1% trifluoroacetic acid in water, eluent B is methanol (100%). Eluent flow rate is set to 0.5 mL/min. Elution with 75% eluent B in the first 2 min is followed by a 2.5 min phase with 100% eluent B. From minute 4.5–8.5 the eluent system is changed back to the original composition of 75% eluent B.

Detection and quantification of 16β-hydroxyprogesterone (first peak), 17β-hydroxyprogesterone (second peak) and progesterone (third peak) are performed using a radioflow detector (Raytest GmbH, Straubenhardt).

Percent inhibition is calculated according equations 1 and 2:

$$\text{conversion} = 100\% \times \frac{\text{area}(16\alpha - \text{hydroxyprogesterone} + 17\alpha - \text{hydroxyprogesterone})}{\text{area}(16\alpha - \text{hydroxyprogesterone} + 17\alpha - \text{hydroxyprogesterone} + \text{progesterone})} \quad (1)$$

$$\% \text{ inhibition} = 100\% - \frac{\text{conversion_with_inhibitor} \times 100\%}{\text{conversion_without_inhibitor}} \quad (2)$$

4.2.3. CYP19 inhibition assay

4.2.3.1. *Preparation of aromatase.* The enzyme was obtained from the microsomal fraction of freshly delivered human term placental tissue according to the procedure of Thompson and Siiteri [33]. The isolated microsomes were suspended in a minimum volume of phosphate

buffer (0.05 M, pH 7.4, 20% glycerol). Additionally, DTT (dithiothreitol, 10 mM) and EDTA (1 mM) were added to protect the enzyme from degradation. The enzyme preparation was stored at –70 °C.

4.2.3.2. *Inhibition of aromatase.* The assay was performed monitoring enzyme activity by measuring the 3H₂O formed from [1β-³H] androstenedione during aromatization. Each incubation tube contained 15 nM [1β-³H]androstenedione (0.08 µCi), 485 nM unlabeled androstenedione, 2 mM NADP, 20 mM glucose-6-phosphate, 0.4 units of glucose-6-phosphate-dehydrogenase and inhibitor (in at least three different concentrations for determining the IC₅₀ value) in phosphate buffer (0.05 M, pH 7.4). The test compounds were dissolved in DMSO and diluted with buffer. The final DMSO concentration in the control and inhibitor incubation was 2%. Each tube was preincubated for 5 min at 30 °C in a water bath. Microsomal protein was added to start the reaction (0.1 mg). The total volume for each incubation was 0.2 mL. The reaction was terminated by the addition of 200 µl of a cold 1 mM HgCl₂ solution. After addition of 200 µl of an aqueous dextran-coated charcoal (DCC) suspension (2%), the vials were shaken for 20 min and centrifuged at 1500× g for 5 min to separate the charcoal-absorbed steroids. The supernatant was assayed for 3H₂O by counting in a scintillation mixture using a β-counter. The calculation of the IC₅₀ values was performed by plotting the percent inhibition vs. the concentration of inhibitor on a semi-log plot. From this the molar concentration causing 50% inhibition was calculated.

Author contributions

AS, AC and RWH conceived the research project and wrote the paper. AS, LP, MC and FL synthesized the known and new CYP inhibitors. SC developed the analytical methods to separate reaction mixtures and check the purity of the new compounds. ON supported molecular design studies and reviewed the manuscript. NH performed all the biological assays. All authors have given approval to the final version of the manuscript.

Funding sources

The Italian authors gratefully acknowledge the support of the project by the University of Bari (Progetti di Ateneo 2012–2013).

Acknowledgments

We thank Marica Mariano, and Chiara Scarabaggio for the preparation of compounds **21** and **22** and Dr Christina Zimmer for

performing some in vitro inhibition assays. We also thank the University of Bari for the support of M.M. and C.S. within the LLP Erasmus project.

References

- [1] D.F. Lewis, *Guide to Cytochrome P450 Structure and Function*, Taylor and Francis eds, London, 2001.
- [2] D.F. Lewis, Y. Ito, P.S. Goldfarb, *Cytochrome P450 structures and their substrate interactions*, *Drug Dev. Res.* 66 (2006) 19–24.

- [3] P. Brown, Prevention: targeted therapy-anastrozole prevents breast cancer, *Nat. Rev. Clin. Oncol.* 11 (2014) 127–128.
- [4] S. George, Y. Feng, J. Manola, M.R. Nucci, J.E. Butrynski, J.A. Morgan, N. Ramaiya, R. Quek, R.T. Penson, A.J. Wagner, D. Harmon, G.D. Demetri, C. Krasner, Phase 2 trial of aromatase inhibition with letrozole in patients with uterine leiomyosarcomas expressing estrogen and/or progesterone receptors, *Cancer* 120 (2013) 738–743.
- [5] P. Carlini, E. Bria, D. Giannarelli, G. Ferretti, A. Felici, P. Papaldo, A. Fabi, C. Nistico, S. Di Cosimo, E.M. Ruggeri, M. Milella, M. Mottotese, E. Terzoli, F. Cognetti, New aromatase inhibitors as second-line endocrine therapy in postmenopausal patients with metastatic breast carcinoma: a pooled analysis of the randomized trials, *Cancer* 104 (2005) 1335–1342.
- [6] S.M. Hoy, Abiraterone acetate: a review of its use in patients with metastatic castration-resistant prostate cancer, *Drugs* 73 (2013) 2077–2091.
- [7] R. Hartmann, U.E. Hille, C. Zimmer, C.A. Vock, Q. Hu, Selective CYP11B1 Inhibitors for the Treatment of Cortisol Dependent Diseases, April 26th, 2012. WO2012052540.
- [8] U.E. Hille, C. Zimmer, J. Hauptenthal, R.W. Hartmann, Optimization of the first selective steroid-11 β -hydroxylase (CYP11B1) inhibitors for the treatment of cortisol dependent diseases, *ACS Med. Chem. Lett.* 2 (2011) 559–564.
- [9] U.E. Hille, C. Zimmer, C.A. Vock, R.W. Hartmann, First selective CYP11B1 inhibitors for the treatment of cortisol-dependent diseases, *ACS Med. Chem. Lett.* 2 (2011) 2–6.
- [10] E.L. Meredith, G. Ksander, L.G. Monovich, J.P.N. Papillon, Q. Liu, K. Miranda, P. Morris, C. Rao, R. Burgis, M. Capparelli, Q.-Y. Hu, A. Singh, D.F. Rigel, A.Y. Jeng, M. Beil, F. Fu, C.-W. Hu, D. LaSala, Discovery and in vivo evaluation of potent dual CYP11B2 (Aldosterone synthase) and CYP11B1 inhibitors, *ACS Med. Chem. Lett.* 4 (2013) 1203–1207.
- [11] Q. Hu, L. Yin, R.W. Hartmann, Aldosterone synthase inhibitors as promising treatments for mineralocorticoid dependent cardiovascular and renal diseases, *J. Med. Chem.* (2014), <http://dx.doi.org/10.1021/jm401430>.
- [12] M.A. Pinto-Bazurco Mendieta, Q. Hu, M. Engel, R.W. Hartmann, Highly potent and selective nonsteroidal dual inhibitors of CYP17/CYP11B2 for the treatment of prostate cancer to reduce risks of cardiovascular diseases, *J. Med. Chem.* 56 (2013) 6101–6107.
- [13] N. Strushkevich, A.A. Gilep, L. Shen, C.H. Arrowsmith, A.M. Edwards, S.A. Usanov, H.W. Park, Structural insights into aldosterone synthase substrate specificity and targeted inhibition, *Mol. Endocrinol.* 27 (2013) 315–324.
- [14] J. Emmerich, Q. Hu, N. Hanke, R.W. Hartmann, Cushing's syndrome: development of highly potent and selective CYP11B1 inhibitors of the (pyridylmethyl)pyridine type, *J. Med. Chem.* 56 (2013) 6022–6032.
- [15] L. Yin, S. Lucas, F. Maurer, U. Kazmaier, Q. Hu, R.W. Hartmann, Novel imidazol-1-ylmethyl substituted 1,2,5,6-tetrahydro-pyrrolo[3,2,1-ij]quinolin-4-ones as potent and selective CYP11B1 inhibitors for the treatment of Cushing's syndrome, *J. Med. Chem.* 55 (2012) 6629–6633.
- [16] D.E. Scheingart, Drugs in the medical treatment of Cushing's syndrome, *Expert Opin. Emerg. Drugs* 14 (2009) 661–671.
- [17] M. Fleseriu, S. Petersenn, Medical management of Cushing's disease: what is the future? *Pituitary* 15 (2012) 330–341.
- [18] L. Roumen, M.P. Sanders, K. Pieterse, P.A. Hilbers, R. Plate, E. Custers, M. de Gooyer, J.F. Smits, I. Beugels, J. Emmen, H.C. Ottenheijm, D. Laysen, J.J. Hermans, Construction of 3D models of the CYP11B family as a tool to predict ligand binding characteristics, *J. Comput. Aided Mol. Des.* 21 (2007) 455–471.
- [19] N.V. Belkina, M. Lisurek, A.S. Ivanov, R. Bernhardt, Modelling of three-dimensional structures of cytochromes P450 11B1 and 11B2, *J. Inorg. Biochem.* 87 (2001) 197–207.
- [20] S. Ulmschneider, M. Negri, M. Voets, R.W. Hartmann, Development and evaluation of a pharmacophore model for inhibitors of aldosterone synthase (CYP11B2), *Bioorg. Med. Chem. Lett.* 16 (2006) 25–30.
- [21] S. Lucas, M. Negri, R. Heim, C. Zimmer, R.W. Hartmann, Fine-tuning the selectivity of aldosterone synthase inhibitors: structure–activity and structure–selectivity insights from studies of heteroaryl substituted 1,2,5,6-tetrahydropyrrolo[3,2,1-ij]quinolin-4-one derivatives, *J. Med. Chem.* 54 (2011) 2307–2319.
- [22] S. Lucas, R. Heim, M. Negri, I. Antes, C. Ries, K.E. Schewe, A. Bisi, S. Gobbi, R.W. Hartmann, Novel aldosterone synthase inhibitors with extended carbocyclic skeleton by a combined ligand-based and structure-based drug design approach, *J. Med. Chem.* 51 (2008) 6138–6149.
- [23] S. Lucas, R. Heim, C. Ries, K.E. Schewe, B. Birk, R.W. Hartmann, In vivo active aldosterone synthase inhibitors with improved selectivity: lead optimization providing a series of pyridine substituted 3,4-dihydro-1*H*-quinolin-2-one derivatives, *J. Med. Chem.* 51 (2008) 8077–8087.
- [24] S. Gobbi, Q. Hu, M. Negri, C. Zimmer, F. Belluti, A. Rampa, R.W. Hartmann, A. Bisi, Modulation of cytochromes P450 with xanthone-based molecules: from aromatase to aldosterone synthase and steroid 11 β -hydroxylase inhibition, *J. Med. Chem.* 56 (2013) 1723–1729.
- [25] R. Heim, S. Lucas, C.M. Grombein, C. Ries, K.E. Schewe, M. Negri, U. Müller-Vieira, B. Birk, R.W. Hartmann, Overcoming undesirable CYP1A2 inhibition of pyridyl-naphthalene-type aldosterone synthase inhibitors: influence of heteroaryl derivatization on potency and selectivity, *J. Med. Chem.* 51 (2008) 5064–5074.
- [26] F. Leonetti, A. Favia, A. Rao, R. Aliano, A. Paluszczak, R.W. Hartmann, A. Carotti, Design, synthesis, and 3D QSAR of novel potent and selective aromatase inhibitors, *J. Med. Chem.* 47 (2004) 6792–6803.
- [27] A. Stefanachi, A.D. Favia, O. Nicolotti, F. Leonetti, L. Pisani, M. Catto, C. Zimmer, R.W. Hartmann, A. Carotti, Design, synthesis, and biological evaluation of imidazolyl derivatives of 4,7-disubstituted coumarins as aromatase inhibitors selective over 17- α -hydroxylase/C17-20 lyase, *J. Med. Chem.* 54 (2011) 1613–1625.
- [28] QikProp, Version 3.7, Schrödinger, LLC, New York, NY, 2013.
- [29] O. Nicolotti, L. Pisani, M. Catto, F. Leonetti, I. Giangreco, A. Stefanachi, A. Carotti, Discovery of a potent and selective hetero-bivalent AChE inhibitor via bioisosteric replacement, *Mol. Inf.* 30 (2011) 133–136.
- [30] L. Pisani, M. Barletta, R. Soto-Otero, O. Nicolotti, E. Mendez-Alvarez, M. Catto, A. Introcaso, A. Stefanachi, S. Cellamare, C. Altomare, A. Carotti, Discovery, biological evaluation, and structure-activity and -Selectivity relationships of 6'-Substituted (E)-2-(Benzofuran-3(2*H*)-ylidene)-*N*-methylacetamides, a novel class of potent and selective monoamine oxidase inhibitors, *J. Med. Chem.* 56 (2013) 2651–2664.
- [31] S.P. Felter, J.D. Vassallo, B.D. Carlton, G.P. Daston, A safety assessment of coumarin taking into account species-specificity of toxicokinetics, *Food Chem. Toxicol.* 44 (2006) 462–475.
- [32] P.B. Ehmer, J. Jose, R.W. Hartmann, J. Steroid Biochem, Development of a simple and rapid assay for the evaluation of inhibitors of human 17 α -hydroxylase-C17,20-lyase (P450c17) by coexpression of P450c17 with NADPH-cytochrome-P450-reductase in *Escherichia coli*, *Mol. Biol.* 75 (2000) 57–63.
- [33] E.A. Thompson, P.K. Siiteri, Utilization of oxygen and reduced nicotinamide adenine dinucleotide phosphate by human placental microsomes during aromatization of androstenedione, *J. Biol. Chem.* 249 (1974) 5364–5372.